KIEL-UP • DOI: 10.38072/2748-3150/p43

Neutron monitor yield function: improved spectral computations of the Forbush decrease of June 2015

Maria Livada, Loukas Xaplanteris, Nafsika Dimosthenous, Helen Mavromichalaki

Correspondence

Nuclear and Particle Physics Department, Faculty of Physics, National and Kapodistrian University of Athens, Greece, mairiliv@phys.uoa.gr, ksaplant@phys.uoa.gr, ndimosthen@phys.uoa.gr, emavromi@phys.uoa.gr

Keywords

galactic cosmic rays; spectral analysis; Forbush decreases; yield functions; neutron monitors

Abstract

In this work a new improved coupling function by Xaplanteris et al. (2021) based on Quantum Field Theory is applied for spectral analysis of cosmic rays. This new coupling function had already been confirmed in the application of cosmic rays with the calculation of primary cosmic ray intensity during Forbush decreases and ground level enhancements but this is the first time that it is used for the calculation of spectral index. To describe the rigidity spectrum of the galactic cosmic ray (GCR) during a Forbush decrease, a power law in rigidity is often used. The exponent of this power law, the spectral index, describes the hardness of the GCR spectrum. The spectrum of the GCR becomes harder during the Forbush decrease main phase. For this analysis the Forbush decrease of the cosmic ray intensity observed on June 2015 was chosen. Daily cosmic ray data of the neutron monitor stations obtained from the high-resolution neutron monitor database (NMDB) were used for calculating the cosmic ray density and anisotropy variations. For the spectral analysis of the galactic cosmic rays the technique of Wawrzynczak and Alania (2010) is applied, based on the coupling coefficient method. The obtained results of the Fd analysis by using the new coupling function by Xaplanteris et al. (2021) are compared with the results obtained based on the coupling function by Clem and Dorman (2000).

1. Introduction

Cosmic rays (CRs) that arrive at the top of the atmosphere are called primary cosmic rays. The cosmic rays that manage to penetrate the Earth atmosphere interact with its components and produce showers of secondary particles that are measured by the ground based detectors. The worldwide network of standard

KIEL-UP • DOI: 10.38072/2748-3150/p43

neutron monitors (NMs) is of great importance for the detection and provision data of secondary neutrons produced by the interaction of cosmic rays and solar energetic particles with the atmospheric molecules to analyze CR variability (Shea & Smart 2000; Moraal et al. 2000).

The linking of the intensity of primary CRs with the NM count rates (secondary cosmic rays) requires high numerical simulations of the atmospheric cascade. One way to achieve this is with the NM yield function and it is crucial for Space Weather research. The yield function of a specific primary particle type is defined as the detector's response to this particle type at energy E and has dimensions of (counts m² sr), so it depends on the geometric characteristics of the NM detector. On the other hand the coupling function is defined as the differential count rate of the NM and has dimensions of counts $(\mathrm{GeV})^{-1}$ (Clem and Dorman 2000). There are several yield functions (or coupling function), some of which are calculated based on theoretical tools while others are defined by statistical and computational models. The FLUKA (Fasso et al. 1993) Monte-Carlo package was used by Clem and Dorman (2000) for simulations of particles transport through the atmosphere. The GEANT-4 (Agostinelli et al. 2003) Monte Carlo package was applied by Flückiger et al. (2008) and Matthiä et al. (2009) for the same reason. Also the GEANT-4 PLANETOCOSMICS Monte-Carlo tool and a realistic atmospheric model were used by Mishev et al. (2013) for the computation of an improved yield function. Recently, a new coupling function based on Quantum Field Theory (QFT) computations was published (Xaplanteris et al. 2021). Yield functions developed by different groups show different results in some energy regions due to the fact that they differ on the set of assumptions they are based on, the processes they take into account and the technique they are derived from (Heck 2006). The necessity of an accurate and suitable yield function has been presented in various publications (e.g. Clem & Dorman 2000; Mavromichalaki et al. 2012) especially for spectral analysis of important events of CRs such as Forbush decreases (Fds) and ground level enhancements (GLEs). In this work we focus on the case of Fds of GCRs.

Forbush decrease manifests itself in the fast decreases of the GCR intensity followed by a gradual recovery phase that happens over 8-10 days (Forbush 1954). Most of Fds occur due to coronal mass ejections (CMEs) which come from the Sun along with a shock wave (Cane 2000; Papailiou et al. 2013). The amplitude of the Fd (%) for each NM is defined as the difference between the cosmic ray intensity at the onset and the minimum point of this. A dependence of the observed difference on the GCR rigidity is one of the fundamental characteristics of Fds. It is given by Cane (2000) and can be expressed by a power law $R^{-\gamma}$, where γ is the spectral index.

In this work we focus on the calculation of the spectral index during the Fd using the technique of Wawrzynczak and Alania (2010) which is based on the coupling coefficient method (Clem and Dorman 2000), secondary cosmic ray measurements can be linked to the primary incident cosmic ray particles via specific mathematical functions. The Fd that took place on 22 June 2015 is studied and analyzed. For spectral analysis two coupling functions were applied to the case of the above Fd, the recently established coupling function based on QFT calculations (Xaplanteris et al. 2021) and the total response function of Clem and Dorman (2000). Our results are discussed.

2. Data selection

In this work daily cosmic ray data corrected for pressure and efficiency from middle latitude NM stations located over the world and obtained from the high resolution real time Neutron Monitor Database (NMDB) (http://www.nmdb.eu) were used. This study analyzes data from five stations with cut-off rigid-

KIEL-UP • DOI: 10.38072/2748-3150/p43

ities above 1.67GV due to the limitations of the QFT coupling function: (Baksan (BKSN) – *R*c = 5.60 GV, Guadalajara (CALM) – *R*c = 6.95 GV, Lomnicky Stit (LMKS) – *R*c = 3.84 GV, Rome (ROME) – *R*c =6.27 GV, Jungfraujoch (JUNG1) – *R*c = 4.5 GV).

The cosmic ray intensity recorded at each station was normalized according to Equation 1:

$$J_i^k = \frac{N_K - N_0}{N_0} \tag{1}$$

where J_i^k is the normalized cosmic ray intensity for the i^{th} station of the Fd, N_k is the daily cosmic ray intensity of each station for k days (k=1,2,3,..days) and N_0 is the average cosmic ray intensity for three days before the beginning of the Fd (Wawrzynczak & Alania 2010). Time profiles of daily values of the cosmic ray intensity of five middle latitude NM stations are presented in (Fig. 1) from 20 June 2015 to 03 July 2015. The first Fd in the studied period happened on 23 June 2015 and had an amplitude with a value of 6.51% for the JUNG1 NM station. The second one took place on 25 June 2015 with an amplitude value of 8.02 % for the LMKS NM station. An increase in the counting rate of the JUNG1 NM station during 29-30 June 2015 (Fig.1) can be explained by the melting snow which may have started even before 29 June 2015 (Maurin et al. 2015) http://cosray.unibe.ch (last accessed May 12, 2023). We plan to make a new Fd analysis and publication in which we will not use the data of JUNG1, but the data of JUNG station.

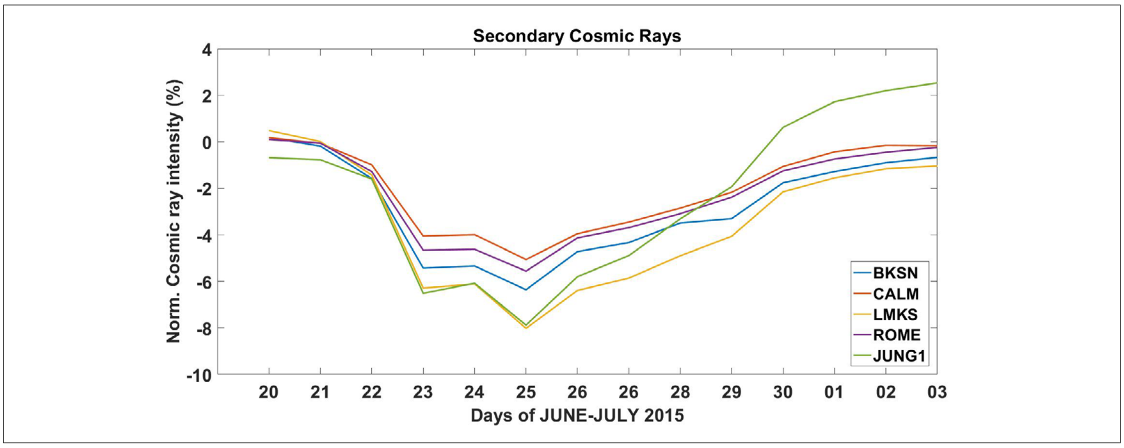

Fig. 1: The normalized CR intensity for middle latitude stations obtained from NMDB for the time period of 20 June 2015 to 03 July 2015.

During the studied period a series of solar events took place on the Sun. In general, 53 C-flares and 7 M-flares occurred on the solar atmosphere and 7 halo and partial halo CMEs at the solar corona, which had a linear velocity up to 1714 km/s. They were observed by GOES and SOHO/LASCO satellites https://www.ngdc.noaa.gov/stp/space-weather/solar-data/; https://cdaw.gsfc.nasa.gov (last accessed September 15, 2022). As for the geomagnetic indices the maximum value of the Kp index was equal to 8 on 22 June 2015 at 18:00-21:00 UT whereas the Dst index had two minimum values: a first one equal to -124nT that was on 22 June 2015 at 21:00-22:00 UT and a second one equal to -204nT that was on 23 June 2015 at 05:00–06:00 UT about a few hours after the minimum of the cosmic ray intensity (Samara et al. 2018) https://www.spaceweatherlive.com ; Final Dst Index Monthly Plot and Table (kyoto-u.ac.jp) (last accessed May 12, 2023). It is thus concluded that two severe G4 geomagnetic storms occurred in the period 22–23 June 2015.

3. Data analysis and results

The method of Wawrzynczak and Alania (2010) used in previous works by Livada et al. (2018) and Livada and Mavromichalaki (2020) for spectral analysis of the Fd events was also applied in this work for the above selected Fds, complemented by the coupling function by Xaplanteris et al. (2021) based on QFT.

According to Wawrzynczak and Alania (2010), secondary cosmic ray data can be linked to the primary incident cosmic ray particles via specific mathematical functions that take into account the acceptance vectors for each detector (NM), based on its local characteristics (cut-off rigidity, altitude, geographic coordinates and detector's type). Each NM station is characterized by its asymptotic cone of acceptance which is a result of the modulation by the geomagnetic field of the cosmic rays (Dorman 2004).

Variations of GCRs intensity near Earth during Fds can be expressed by a power law in rigidity, according to Equation (2):

$$\frac{\delta D(R)}{D(R)} = \begin{cases} A\left(\frac{R}{R_o}\right)^{-\gamma} & R \le R_{max} \\ 0 & R > R_{max} \end{cases} \tag{2}$$

where R_0=10GV and R_{max}=200GV is the rigidity above which the Fd of GCRs vanishes (Dorman 2004).

The cosmic ray intensity J_i^k of the Fd for the i^{th} detector with geomagnetic cut-off rigidity R_i at an atmospheric depth h_i (Dorman 1963) is defined as in Equation (3):

$$J_i^k = \int_{R_i}^{R_{max}} \left(\frac{\delta D(R)}{D(R)}\right)_k W_i(R, h_i)\, \mathrm{d}R \tag{3}$$

where $W_i(R, hi)$ is the coupling coefficient for the NM. In this study two coupling functions were studied the first is by Xaplanteris et al. (2021) and the second by Clem and Dorman (2000) which analyzed in section 3.1 and 3.2.

$$W(E) = 1.65 \times 10^{-2} \frac{1}{E^3} \left[\ln\left(\frac{E}{E_{cut}}\right)\right]^2 \left[\frac{5}{1 - 0.095\ln\left(\frac{E}{E_{cut}}\right)}\right]^2$$ by Xaplanteris et al. (2021)

$$w_T(R, h) = \alpha(h)\,(k(h)-1)\,\exp\left(-a(h)\,R^{-k(h)+1}\right) R^{-K(h)}$$ by Clem and Dorman (2000)

Inserting the power law of Equation (2) into Equation (3) and solving for the cosmic ray intensity of the Fd in free space (in the heliosphere) A_i^k, we can conclude the Equation (4) below:

$$A_i^k = \frac{J_i^k}{\int_{R_i}^{R_{max}} \left(\frac{R}{R_0}\right)^{-\gamma^k} W_i(R, h_i)\, dR} \tag{4}$$

where A_i^k should be independent of the local characteristics of the NM. Yasue et al. (1982) calculated the aforementioned coupling integral for discrete magnitudes and γ. In our analysis the cosmic ray intensity A_i^k of the Fd in the heliosphere was calculated for discrete values of γ ranging from 0.1 to 2 with step 0.01 using Matlab program (201 values) for '*i*' NMs. According to our requirement an acceptable γ_o^{κ} must correspond to the values of the A_i^k being almost the same for all NMs, i.e. $\Delta A_i^k = A_i^k - \bar{A}^k$ should be the minimal value. The errors $\Delta\gamma$ of each spectral index were calculated based on the previous (k-1) and the next value (k+1) of spectral index γ_o.

KIEL-UP • DOI: 10.38072/2748-3150/p43

The technique of Wawrzynczak and Alania (2010) is based on the coupling function $W_i(R, h_i)$ between the intensity of NMs J_i^k and the primary cosmic rays A_i^k in the heliosphere that was described from Equation 4. In this work two types of coupling coefficient expressions are obtained.

3.1 Theoretical coupling function

The first theoretical coupling function is the one proposed by Xaplanteris et al. (2021). It is derived purely analytically and aims to test the applicability of QFT computational tools to CRs phenomena. Initially a slight variation of the Lagrangian density L of a traditional Φ^4 theory is chosen (Peskin & Schroeder 1995; Srednicki 2007; Bilal 2011):

$$L = \tfrac{1}{2}\left(\partial_\mu \Phi_1\right)^2 + \tfrac{1}{2}\left(\partial_\mu \Phi_2\right)^2 + \tfrac{1}{2}m_1^2\Phi_1^2 + \tfrac{1}{2}m_2^2\Phi_2^2 - \tfrac{\lambda}{2!2!}\Phi_1^2\Phi_2^2 \tag{5}$$

where Φ_1 and Φ_2 are scalar fields that describe the proton of mass m_1 and the neutron of mass m_2 respectively and are coupled with a coupling constant λ.

The interaction resulting in neutron production assumes that a primary proton, moving towards the Earth's surface, collide with a large atmospheric particle X and as a result a secondary proton (less energetic than the initial one) is produced alongside with a neutron and a large particle A. The large atmospheric particle X refers to an atmospheric molecule with large enough mass compared to the mass of a nucleon, so that in the equation of energy conservation it can be assumed at rest. More specifically in the calculation of the scattering amplitude using the Lehmann, Symmanzik, Zimmermann (LSZ) formula the particle used as X is nitrogen with mass M=14 m_p=14 GeV (Xaplanteris et al.2021).

$$p^+ + X \rightarrow p^+ + n + A$$

Essentially, the model assumes that the produced neutron escapes from the particle X, meaning that particles X and A have masses differing by 1GeV. Furthermore, the secondary proton and neutron are assumed to travel towards the Earth's surface and particles X and A are considered at rest since their masses are much larger than the nucleons' masses. The final assumption that is made in this model is that after every interaction the secondary proton is left with 60% of its initial energy (Dorman 1974) whereas the remaining 40% is assigned to the neutron and particle A. Therefore, the energy cut-off is 1GeV corresponding to a rigidity cut-off of 1.71GV.

Using QFT principles in order to determine the scattering amplitude for the interaction considered the new coupling function can be derived as an expression of the energy E (Xaplanteris et al.2021):

$$W(E) = 1.65 \times 10^{-2}\tfrac{1}{E^3}\left[\ln\left(\tfrac{E}{E_{cut}}\right)\right]^2\left[\tfrac{5}{1-0.095\ln\left(\frac{E}{E_{cut}}\right)}\right]^2 \tag{6}$$

where E denotes the energy of the initial proton, E_{cut} = *1 G*eV (or R_{cut} =1.71 GV). This means that it can take into account incident protons with energy greater than *1 Ge*V. This limitation renders the coupling function applicable only to NM stations with energy cut-off value greater than *1 Ge*V.

It is important to note that the coupling function is not normalized since it can only be applied for energies $E \geq 1$ *G*eV and does not consider inelastic processes, thermalization and diffusion.

KIEL-UP • DOI: 10.38072/2748-3150/p43

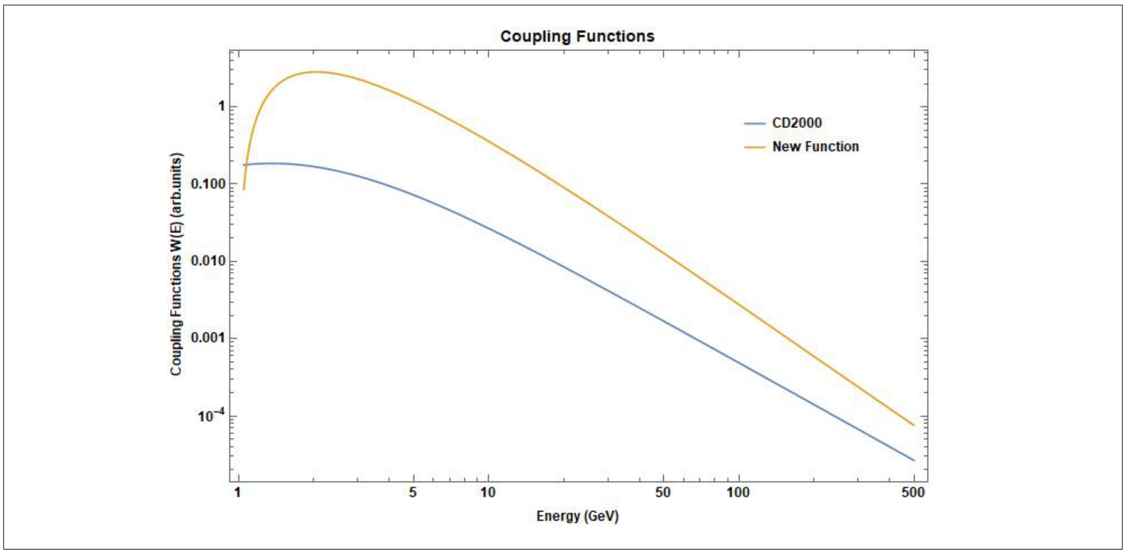

Fig. 2: Comparison of the newly computed coupling function based on QFT (Xaplanteris et al. 2021) with the function of Clem and Dorman (2000).

3.2 Total response function

The second coupling function is the total response function of Clem and Dorman (2000) given in Equation (7).

$$w_T(R, h) = \alpha(h)\,(k(h)-1)\,\exp\left(-a(h)\,R^{-k(h)+1}\right) R^{-K(h)} \tag{7}$$

where R is the cut-off rigidity of each station and α and κ are depth-dependent parameters which depend on solar activity (minimum or maximum).

In Fig. 2 the yield function of QFT (Xaplanteris et al. 2021) and the function of Clem and Dorman (2000) where the fit is adapted from Caballero-Lopez and Moraal (2012) are compared. The two curves follow the same behavior with a significant deviation in the lower energies between 2 GeV and 10 GeV. A more detailed justification between the new QFT coupling function and with other ones is given in the work of Xaplanteris et al. (2021).

4. Discussion and conclusions

The method of Wawrzynczak and Alania (2010) was applied using the above two coupling functions according to QFT (Xaplanteris et al. 2021) and Clem and Dorman (2000) respectively, for the calculation of cosmic ray intensity in the heliosphere near Earth for each station and the spectral index during the Fd of June 2015. For the calculation the daily data of five NM stations were used. In Figs. 3 and 4 the results of our calculations are presented.

- From our analysis it is concluded that during the events of June 2015, a temporal continuity between the solar events and the associated phenomena that were recorded on the Earth, exists. The observed Fds are directly associated with the production of CMEs on the Sun and the created shock waves.

KIEL-UP • DOI: 10.38072/2748-3150/p43

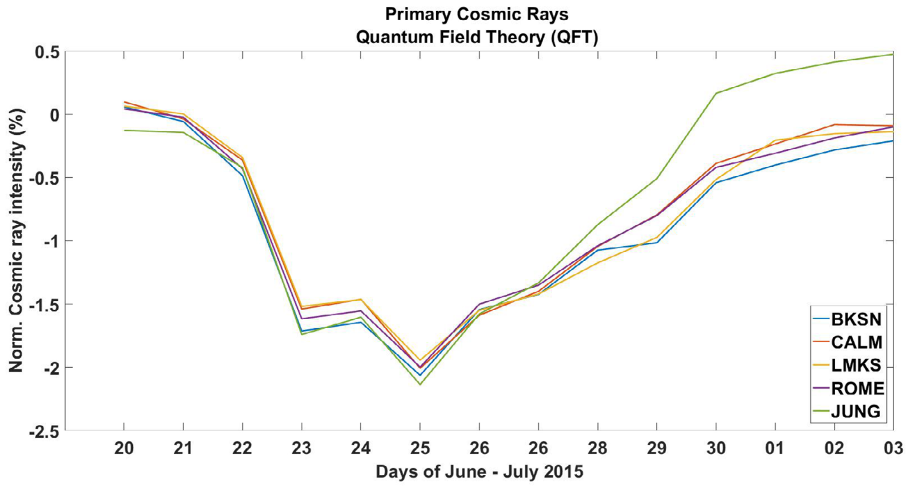

Fig. 3: Time profiles of the primary cosmic ray variations applying the coupling function of Xaplanteris et al. (2021) (above panel) and the function of Clem and Dorman (2000) (down panel) for the time period of 20 June 2015–03 July 2015.

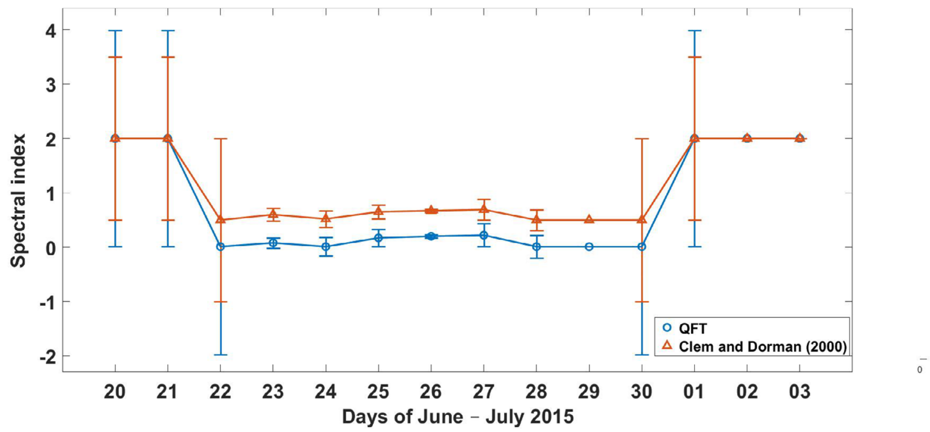

Fig. 4: Temporal changes of the rigidity spectrum exponent applying the coupling function of Xaplanteris et al. (2021) (blue line) and the function of Clem and Dorman (2000) (red line) for the time period of 20 June 2015 – 03 July 2015.

- According to the method of Wawrzynczak and Alania (2010) the calculated intensity of the primary cosmic rays is expected to be almost the same for the selected NMs due to the fact that it does not depend on the local characteristics of the detectors. This statement was confirmed by the two above coupling functions in Fig. 3 in the case of the selected Fd. In contrast the intensity of the secondary cosmic rays has different values in each station, with some stations having larger amplitude than others stations due to their cut-off rigidity (Fig. 1). However, the primary normalized cosmic ray intensity has difference when determined by the coupling function of Xaplanteris et al. (2021) and by the function of Clem and Dorman (2000) as well as the maximum GCR decrease is ~2% for the results of first coupling function and ~12% for the second Fig. 3. This is caused due to the fact that the calculated cosmic ray intensity depends on the using of coupling function. The newly computed function takes higher values for the energy region under study than the Clem and Dorman (2000) Fig. 2.

- The purpose of this work is to show that the time dependence of the calculated spectral index is in agreement with the fluctuations of the cosmic ray intensity during the Fds (Livada and Mavromichalaki 2020). This is achieved for the Fd of June 2015 for both coupling functions used. Specifically, the spectral index reached the minimum value during the main phase of Fd with the largest amplitude of the Fd (Fig. 4). It means that the spectrum of the GCR becomes harder during the Fd main phase. The deviations of the value of the daily spectral index are within the limit of the calculated error $\Delta\gamma$. In Fig. 4 and Tab. 1 the comparison of the results of the calculated spectral index with both cases of coupling functions is presented, in order to confirm that the new function produces similar results to the other.

Tab. 1: Daily values of the spectral index with the errors for the time period 20 June 2015–03 July 2015.

Date YYYY:MM:DD	Spectral index QFT (Xaplanteris et al. 2021)	Spectral index (Clem & Dorman 2000)
2015:06:20	2.00 ±1.99	2.00±1.50
2015:06:21	2.00±1.99	2.00±1.50
2015:06:22	0.01±1.99	0.50±1.50
2015:06:23	0.08±0.09	0.60±0.12
2015:06:24	0.01±0.17	0.52±0.15
2015:06:25	0.17±0.16	0.65±0.13
2015:06:26	0.20±0.03	0.67±0.03
2015:06:27	0.22±0.21	0.69±0.19
2015:06:28	0.01±0.21	0.50±0.19
2015:06:29	0.01±0.00	0.50±0.00
2015:06:30	0.01±1.99	0.50±1.50
2015:07:01	2.00±1.99	2.00±1.50
2015:07:02	2.00±0.00	2.00±0.00
2015:07:03	2.00±0.00	2.00±0.00

Acknowledgements

Special thanks are due to our colleagues of the Neutron Monitor stations (www.nmdb.eu) for kindly providing the cosmic ray data used in this study in the frame of the High resolution Neutron Monitor database NMDB, funded under the European Union's FP7 Program (contract no. 213007). Athens neutron Monitor station is supporting by the Special research account of the National and Kapodistrian University of Athens. Thanks are due to the IZMIRAN group of the Russian Academy of Sciences for kindly providing the Forbush decrease data.

KIEL-UP • DOI: 10.38072/2748-3150/p43

References

Agostinelli, S., Allison, J., Amako, k., Apostolakis, J., Araujo, H., et al. 2003, Geant4- a simulation toolkit, Nucl Instr. Meth. Phys. Res. A, 506, 250-303, https://doi.org/10.1016/S0168-9002(03)01368-8

Bilal, A. 2011, Advanced quantum field theory: renormalization, non-abelian gauge theories and anomalies. In: Lect. Notes Brus.

Caballero-Lopez, R.A., Moraal, H. 2012, Cosmic-ray yield and response functions in the atmosphere. J. Geophys. Res. Space Phys. 117, A12103, https://doi.org/10.1029/2012JA017794

Cane, H.V. 2000, Coronal Mass Ejections and Forbush Decreases. Space Sci. Rev. 93, 55-77, https://doi.org/10.1023/A:1026532125747

Clem, J.M., Dorman, L.I. 2000, Neutron Monitor Response Functions. Space Sci. Rev. 93, 335–359, https://doi.org/10.1023/A:1026508915269

Dorman, L.I. 2004, Cosmic Rays in the Earth's Atmosphere and Underground. Kluwer Academic Publishers, Dordrecht, https://doi.org/10.1007/978-1-4020-2113-8

Dorman, L.I. 1974, Cosmic Rays Variations and Space Explorations. North-Holland, Amsterdam.

Dorman, L.I. 1963, Cosmic Rays Variations and Space Exploration. Nauka, Moscow.

Flückiger, E.O., Moser, M.R., Pirard, B., Bütikofer, R., Desorgher, L. 2008, A parameterized neutron monitor yield function for space weather applications. Proc. 30th ICRC Mexico, ed. by R. Caballero, J. D'Olivo, G. Medina-Tanco, L. Nellen, F. Sánchez, and J. Valdés-Galicia, 1, 289–292, https://indico.nucleares.unam.mx/event/4/session/78/contribution/1182/material/paper/0.pdf (last accessed July 4, 2023).

Fasso, A., Ferrari, A., Ranft, A., Sala, P. R., Stevenson, G. R., and Zazula, J.M. 1993, A comparison of Fluka Simulations with measurements of Fluence and Dose in Calorimeter structures, Nucl. Inst. Meth. A332,459-468, https://doi.org/10.1016/0168-9002(93)90301-W

Forbush, S. E. 1954, World-wide cosmic-ray variations, 1937–1952. J. Geophys. Res. 59, 525–542, https://doi.org/10.1029/JZ059i004p00525

Heck, D. 2006, Low-energy hadronic interaction models. Nucl. Phys. B-Proc. Suppl. 151, 127–134, https://doi.org/10.1016/j.nuclphysbps.2005.07.024

Livada, M., Mavromichalaki, H. 2020, Spectral Analysis of Forbush Decreases Using a New Yield Function. Solar Phys. 295(115), https://doi.org/10.1007/s11207-020-01679-z.

Livada, M., Mavromichalaki, H., Plainaki, C. 2018, Galactic cosmic ray spectral index: the case of Forbush decreases of March 2012. Astrophys. Space Sci. 363(8), https://doi.org/10.1007/s10509-017-3230-9.

Matthiä, D., Heber, B., Reitz, G., Meier, M., Sihver, L., Berger, T., Herbst K. 2009, Temporal and spatial evolution of the solar energetic particle event on 20 January 2005 and resulting radiation doses in aviation. J. Geophys. Res. 114(A08104), https://doi.org/10.1029/2009JA014125

Maurin, D., Cheminet, A., Derome, L., Ghelfi, A., Hubert, G. 2015, Neutron monitors and muon detectors for solar modulation studies: interstellar flux, yield function, and assessment of critical parameters in count rate calculations. Adv. Space Res. 55, 363-389, https://doi.org/10.1016/j.asr.2014.06.021

Mavromichalaki, H. 2012, The physics of cosmic rays applied to space weather. Advances in Solar and Solar-Terrestrial Physics, ed. by G. Maris, C. Demetrescu, 135–161.

Mishev, A.L., Usoskin, I.G., Kovaltsov, G.A. 2013, Neutron monitor yield function: New improved computations. J. Geophys. Res. 118, 2783–2788, https://doi.org/10.1002/jgra.50325

Moraal, H., Belov, A., Clem, J. M. 2000, Design and co-Ordination of Multi-Station International Neutron Monitor Networks. Space Sci. Rev. 93, 285–303, https://doi.org/10.1023/A:1026504814360

Papailiou, M., Mavromichalaki, H., Abunina, M., Belov, A., Eroshenko, E., Yanke, V., Kryakunova, O. 2013, Forbush Decreases Associated with Western Solar Sources and Geomagnetic Storms: A Study on Precursors. Solar Phys. 283, 557–563, https://doi.org/10.1007/s11207-013-0231-x

Peskin, M.E., Schroeder, D.V. 1995, An Introduction to Quantum Field Theory. Perseus Books, Cambridge.

Samara, E., Smponias, A., Lytrosyngounis, I., Lingri, D., Mavromichalaki, H., Sgouropoulos, C. 2018, Unusual Cosmic Ray Variations During the Forbush Decreases of June 2015. Solar Phys. 293(67), https://doi.org/10.1007/s11207-018-1290-9

Shea, M. A., Smart, D. F. 2000, Fifty Years of Cosmic Radiation Data. Space Sci. Rev. 93, 229–262, https://doi.org/10.1023/A:1026500713452

Srednicki, M. 2007, Quantum Field Theory. Cambridge University Press, Cambridge, https://doi.org/10.2277/0521864496

Wawrzynczak, A., Alania, M.V. 2010, Modeling and data analysis of a Forbush decrease. Adv. Space Res. 45, 622–631, https://doi.org/10.1016/j.asr.2009.09.005

Xaplanteris, L., Livada, M., Mavromichalaki, H., Dorman, L., Georgoulis, M.K., Sarris, T.E. 2021 Improved Approach in the Coupling Function Between Primary and Ground Level Cosmic Ray Particles Based on Neutron Monitor Data. Solar Phys. 296(91), https://doi.org/10.1007/s11207-021-01836-y

Yasue, S., Mori, S., Sakakibara, S. et al. 1982, Coupling coefficients of cosmic rays daily variations for neutron monitors. 7, Nagoya

KIEL-UP • DOI: 10.38072/2748-3150/p43